

## Electronic Supplementary Information

### **Ti<sub>3</sub>C<sub>2</sub>/BiVO<sub>4</sub> Schottky junction as a Signal Indicator for Ultrasensitive Photoelectrochemical Detection of VEGF<sub>165</sub>**

Yaling Liu, Hongmei Zeng, Yaqin Chai, Ruo yuan\*, Hongyan Liu\*

Key Laboratory of Luminescent and Real-Time Analytical Chemistry (Southwest University), Ministry of Education, College of Chemistry and Chemical Engineering, Southwest University, Chongqing 400715, PR China

## 1. EXPERIMENTAL SECTION

### 1.1 Materials and Reagents

Ti<sub>3</sub>AlC<sub>2</sub>, hydrofluoric acid (HF, content ≥ 40.0%), dimethylsulfoxide (DMSO), ethanol and NH<sub>4</sub>VO<sub>3</sub> were purchased from Adamas Reagent Co. Ltd. Bi(NO<sub>3</sub>)<sub>3</sub>·5H<sub>2</sub>O was provided by Shenyang Reagent Fifth Factory. Methylene blue (MB) was purchased from Shanghai Aladdin Industrial Corporation (Shanghai, China). Hydrogen peroxide (H<sub>2</sub>O<sub>2</sub>) was bought from Kelong Chemical Inc. (Chengdu, China). Hexanethiol (HT), gold chloride tetrahydrate (HAuCl<sub>4</sub>·4H<sub>2</sub>O), N-(3-(Dimethylamino)propyl)-N'-ethylcarbodiimide hydrochloride (EDC), N-hydroxy succinimide (NHS) and cetyltrimethyl-ammonium bromide (CTAB) were purchased from Sigma-Aldrich (St. Louis, MO, USA). T7 Exo and 10 × NEbuffer 4 were received from New England Biolabs Ltd. (Beverly, MA, USA). Monodispersed magnetic polystyrene microspheres were purchased from Tianjin Baseline ChromTech Research Centre. Phosphate buffered saline (PBS, pH 7.0) was prepared via dissolving 0.1 M KCl, 0.1 M Na<sub>2</sub>HPO<sub>4</sub> and 0.1 M KH<sub>2</sub>PO<sub>4</sub>. [Fe(CN)<sub>6</sub>]<sup>3-/4-</sup> solution (5.0 mM) was prepared by dissolving potassium ferrocyanide and potassium ferricyanide into 0.1 M PBS solution (pH 7.0). The VEGF<sub>165</sub> and DNA oligonucleotides used in the experiment were synthesized by Sangon Biotech Co. Ltd. (Shanghai, China). The corresponding sequences were listed in Table S1.

### 1.2 Apparatus

The PEC measurement during the experiment was performed on a PEC workstation (Ivium, Netherlands). Electrochemical impedance spectroscopy (EIS),

cyclic voltammetry (CV) measurement and electrochemical deposition were performed on a CHI 660e electrochemical workstation (Shanghai Chenhua Instrument, China). Gel Doc XR<sup>+</sup> System (Bio-Rad, California, USA) was used to take gel-imaging. The morphologies of the prepared nanomaterials were characterized by a scanning electron microscopy (SEM, S-4800, Hitachi, Japan). Powder X-ray diffraction (XRD) patterns were performed on a XD- 3 X-ray diffractometer with Cu K $\alpha$  radiation (Purkinje, China).

**Table S1.** The Oligonucleotide Sequences Used in the Experiment.

Name	Sequence (5'→3')
HP1	GTC TAG CGA CTG AGT TCA GCT AGA CTT TTT TTT TTT TTT TTT T-SH
HP2	TT TTT CTC TTG TCT GGA AGA CGC GTG TCT CCT ATC GTC AGC GGT CAG ACG ATA GCC CGT CTT TCC GTC TTC CAG ACA AGA GTG CAG GG
S1	AA AGA CGG GCT ATC GTC TGA CCG CTG ACG ATA GGA GAC ACG CGT CTT CCA GAC AA-NH <sub>2</sub>
S2	GTC TAG CTG AAC TCA GTC AAG ACG CGT GTC
S3	GTC TAG CTG AAC TCA GTC TAT CGT CAG CGG
S4	GTC TAG CTG AAC TCA GTC GAC GAT AGC CCG

### 1.3 Preparation of the Ti<sub>3</sub>C<sub>2</sub> Sheet

Ti<sub>3</sub>C<sub>2</sub> was prepared according to the previous reported method.<sup>[1,2]</sup> Firstly, 1 g Ti<sub>3</sub>AlC<sub>2</sub> was etched in 20 mL HF solution under constant stirring for 3 days. The precipitate was washed with water and ethanol until the pH  $\geq$  6. The powder was

dired at 70 °C. The  $\text{Ti}_3\text{C}_2$  nanosheets were prepared by subsequent ultrasonic exfoliation. The powder was dispersed in 20 mL DMSO with constant stirring for 24 h at 25 °C. Furthermore, the precipitate was washed by water for several times to remove the redundant DMSO and then sonicated in  $\text{N}_2$  atmosphere for 24 h. Finally, the suspension was centrifuged at 3000 rpm to obtain the product.

#### 1.4 Preparation of the $\text{Ti}_3\text{C}_2/\text{BiVO}_4$

The  $\text{Ti}_3\text{C}_2/\text{BiVO}_4$  was prepared as follows: Briefly, 1 mM  $\text{NH}_4\text{VO}_3$  and 0.02 g CTAB were dissolved in 20 mL water with vigorous stirring for 1 h. Secondly, a certain amount of  $\text{Ti}_3\text{C}_2$  (3.24 mg, 6.48 mg, 16.20 mg) and 1 mM  $\text{Bi}(\text{NO}_3)_3 \cdot 5\text{H}_2\text{O}$  were dissolved in 20 mL water, following by dropping into the  $\text{NH}_4\text{VO}_3$  aqueous solution under continuous stirring. Subsequently, the mixture was transferred into the Teflon-lined stainless-steel autoclave at 180 °C for 12 h. Finally, the product was centrifuged and washed for several times then dried at 70 °C for 12 h.

#### 1.5 T7 Exo-Assisted Target $\text{VEGF}_{165}$ -Induced Dual Signal Amplification

Magnetic bead-S1 was obtained as follows: Firstly, 200  $\mu\text{L}$  of the carboxylated magnetic beads was dispersed in 800  $\mu\text{L}$  PBS (0.1 M, pH 7.0) and washed for three times with water. After that, the cleaned magnetic beads were dispersed in 600  $\mu\text{L}$  PBS containing 11.5 mg EDC and 1.70 mg NHS to active the carboxyl on the surface of magnetic beads, and the solution was gentle stirring for about 40 min at 4 °C. Then amino-modified DNA chain S1 (40  $\mu\text{L}$  of 50  $\mu\text{M}$ ) was dropped into the magnetic beads solution with gentle stirring at 4 °C overnight. To get rid of the redundant S1, the mixture was magnetic separated and washed three times with PBS and

redispersed in 1000  $\mu\text{L}$  PBS. Subsequently, 40  $\mu\text{L}$  of 50  $\mu\text{M}$  S2, S3 and S4 were added into the above mixture to hybrid with S1 for 2 h at 37  $^{\circ}\text{C}$  to obtain magnetic bead-S1-S2-S3-S4, followed by magnetic separation and washing with PBS to remove the extra S2, S3 and S4. On the other hand, HP2 reacted with different concentrations of VEGF<sub>165</sub> for 1 h at 25  $^{\circ}\text{C}$  to form VEGF<sub>165</sub>-HP2 complexes. Next, the VEGF<sub>165</sub>-HP2 complexes were mixed with magnetic bead-S1-S2-S3-S4, so that HP2 can specifically recognize the exposed toehold of S1 and bind to it to release S2, S3, S4. Thus, the output S2, S3, S4 can be used for signal amplification. Later then, the T7 Exo digested S1 from the HP2-S1 hybrid, releasing VEGF<sub>165</sub>-HP2 for the next cycle.

### 1.6 Fabrication of the PEC Biosensor

First of all, the bare GCE was respectively sonicated in ethanol, deionized water and further polished with alumina slurry to obtain clean GCE. Then, 10  $\mu\text{L}$  of 0.5 mg/mL Ti<sub>3</sub>C<sub>2</sub>/BiVO<sub>4</sub> was coated on the electrode surface and dried at room temperature to form a photoactive film. Subsequently, the electrode was immersed in HAuCl<sub>4</sub> (1 %) for electrodeposition under -0.2 V for 10 s to obtain Au NPs. After that, 10  $\mu\text{L}$  of 2  $\mu\text{M}$  HP1 was incubated on the electrode for 12 h at 4  $^{\circ}\text{C}$ . Next, 10  $\mu\text{L}$  HT was modified on the electrode for about 40 min to block the nonspecific binding sites. Then, 10  $\mu\text{L}$  of the output (S2, S3 and S4) was incubated on the electrode for 2 h at 37  $^{\circ}\text{C}$  to form DNA double-chain structure. Finally, 5  $\mu\text{L}$  of 2  $\mu\text{M}$  MB was dropped on the electrode surface and incubated for 1 h.

### 1.7 PEC Measurement Procedure

In this work, the PEC measurement was performed in 5 mL of PBS solution (0.1 M, pH 7.0) within 0.1 M electron donor  $\text{H}_2\text{O}_2$ . The 365 nm excitation light source was provided by the light-emitting diode (LED) lamp and switched off-on-off for 10-20-10 s under 0.0 V potential.

### 1.8 Polyacrylamide Gel Electrophoresis (PAGE)

The strand displacement reaction was investigated by PAGE. Firstly, 2  $\mu\text{L}$  loading buffer solution was added into 10  $\mu\text{L}$  ten DNA samples, respectively. Then, the mixtures were added into ten lanes of freshly prepared polyacrylamide gel (16 %). Subsequently, the electrophoresis was conducted at 120 V in  $1 \times$  TBE buffer for 90 min. Afterwards, the gel was stained by ethidium bromide (EB) solution for 25 minutes and the Molecular Imaging Gel Doc XR system with Image Lab software was used to photograph the image of gel electrophoresis for obtaining electrophoresis results.

### 1.9 Optimization of Experimental Condition

$\text{H}_2\text{O}_2$ , as an electron donor, can provide electrons for photoactive materials, thus promoting the separation of electrons and holes. Therefore, the concentration of  $\text{H}_2\text{O}_2$  can remarkably influence the photocurrent signal. It was worth to explore the optimum concentration of  $\text{H}_2\text{O}_2$  during the test. As shown in Figure S1A, as the concentration of  $\text{H}_2\text{O}_2$  increased, the photocurrent signal continued to increase. When the concentration of  $\text{H}_2\text{O}_2$  was 0.1 M, the photocurrent signal was the strongest. When the concentration exceeded 0.1 M, the photocurrent signal slightly decreased. Thus, the optimum concentration of  $\text{H}_2\text{O}_2$  was 0.1 M in the test. As

shown in Figure S1B, the photocurrent response enhanced visibly along with the concentration of MB increased, while it decreased gradually when the concentration of MB surpassed 0.5 mM. Therefore, 0.5 mM MB was selected as the optimal MB concentration.

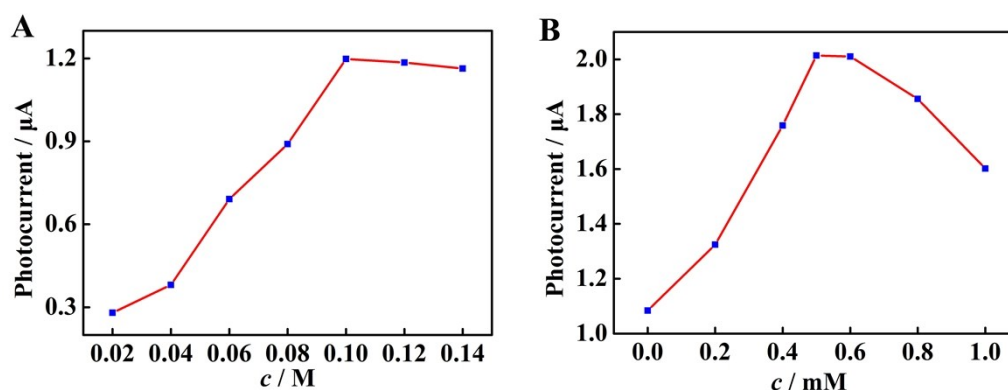


**Figure S1** (A) The PEC responses at different concentrations of  $\text{H}_2\text{O}_2$ ; (B) The PEC responses at different concentrations of MB

The UV-vis spectroscopy of  $\text{Ti}_3\text{C}_2/\text{BiVO}_4$  was shown in Figure S2A. The characteristic absorption peaks of  $\text{Ti}_3\text{C}_2/\text{BiVO}_4$  were located at 273, 365 and 523 nm. The wide range of the absorption band of  $\text{Ti}_3\text{C}_2/\text{BiVO}_4$  indicates that it possesses good photoelectric conversion efficiency. The assay of  $\text{Ti}_3\text{C}_2/\text{BiVO}_4$  was carried out at wavelength of 660 nm, 623 nm, 400 nm, 523 nm, 460 nm and 365 nm, the result showed that the material exhibits photocurrent signals at 400 nm, 523 nm, 460 nm, 365 nm, the irradiation wavelength of 365 nm was optimized (Figure S2B). Therefore, 365 nm light-emitting diode (LED) light was chosen as the excitation light source.

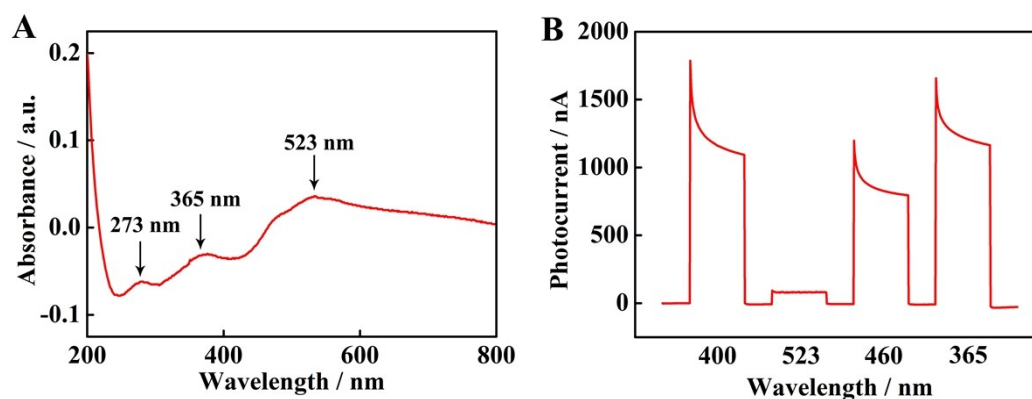


**Figure S2** (A) UV-vis absorption spectra of different materials; (B) The PEC responses at different wavelength.

## 2. RESULTS AND DISCUSSION

### 2.1 Feasibility Investigation of the VEGF<sub>165</sub> Detection

In order to research the feasibility of the biosensor, polyacrylamide gel electrophoresis (PAGE) was used to characterize the process. As shown in Figure S3, lane 1, lane 2, lane 3 and lane 4 represented the DNA S1, S2, S3 and S4. Lane 5 was the hybrid of S1, S2, S3 and S4, which migrated much slower because of the higher molecular weight. The result indicated the successful hybridization of S1, S2, S3 and S4. After the adding of VEGF<sub>165</sub>-HP2 (lane 6), HP2 could specifically recognize the exposed toehold of S1 and hybrid with S1 to form HP2-S1 hybrid (lane 7), thus S2, S3 and S4 could be released. In addition, lane 8 showed a paralleling band to lane 6 and a darker band with the addition of T7 Exo, indicating that the VEGF<sub>165</sub>-HP2 was released digesting of S1 by T7 Exo. HP1 was shown in lane 9. After the hybridization of output DNA S2, S3, S4 and HP1, a slower mobility band compared with lane 9 was observed in lane 10, suggesting the hybridization of S2, S3, S4 with HP1. Therefore,

the results proved the process of target VEGF<sub>165</sub>-induced T7 Exo-assisted dual signal amplification strategy was feasible.

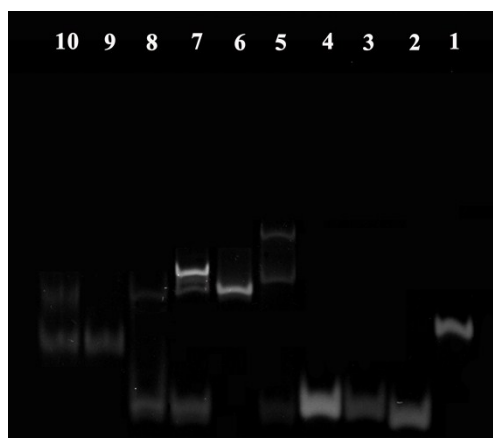


**Figure S3** PAGE analysis with different samples. Lane 1: S1; Lane 2: S2; Lane 3: S3; Lane 4: S4; Lane 5: S1+S2+S3+S4; Lane 6: HP2; Lane 7: HP2+VEGF<sub>165</sub>+S1+S2+S3+S4; Lane 8: T7 Exo+HP2+VEGF<sub>165</sub>+S1+S2+S3+S4; Lane 9: HP1; Lane 10: HP1+T7 Exo+HP2+VEGF<sub>165</sub>+S1+S2+S3+S4.

## 2.2 Characterizations of the Biosensor

To investigate the construction of the PEC biosensor, the assembly process was characterized by cyclic voltammetry (CV) measurement and electrochemical impedance spectroscopy (EIS). As shown in Figure S4A, after Ti<sub>3</sub>C<sub>2</sub>/BiVO<sub>4</sub> was coated (curve b), there was an apparently decrease of the peak current compared with the bare GCE (curve a). The peak current was enhanced obviously because of the deposition of Au nanoparticles. When HP1 was incubated on the electrode (curve d), the peak current decreased due to the hindered electron transfer. Additionally, a further decrease of the current was observed accounting for the blocking effect of Hexanethiol (HT) (curve e). When the electrode was incubated with S2, S3, S4 and MB (curve f), there was an enhancement of the peak current because MB can

facilitate electron transfer to the electrode surface. Figure S4B shows the semicircle diameter equals electron transfer resistance ( $R_{et}$ ) of the electrode, there was a small semicircle of the bare electrode (curve a). The  $R_{et}$  was enhanced after  $Ti_3C_2/BiVO_4$  was coated on the electrode (curve b). When the electrode surface was modified with Au NPs, the  $R_{et}$  decreased obviously because of the conductive Au NPs (curve c). The  $R_{et}$  successively increased when HP1 (curve d) and HT (curve e) were incubated on the electrode because HT and negatively charged DNA can hinder charge transfer. Subsequently, the  $R_{et}$  apparently decreased after S2, S3, S4 and MB were incubated (curve f), since MB could be beneficial to transport electrons along the dsDNA.

In addition, PEC characterization was used for investigating the assembly process of the biosensor (Figure S4C). The photocurrent signal was nearly zero for the bare GCE (curve a). After  $Ti_3C_2/BiVO_4$  was coated on the electrode, the initial photocurrent was obtained (curve b). When Au NPs were electrodeposited on the electrode (curve c), the PEC response was further enhanced because of the conductivity of Au NPs. However, the PEC response was continuously declined after HP1 (curve d) and HT (curve e) were modified on the electrode, owing to the poor electrons transfer ability of DNA and HT. Finally, with the addition of the output DNA and MB (curve f), the photocurrent was enhanced, due to the fact that MB can increase the light absorption and promote the electron transfer along the dsDNA to generate a higher photocurrent.

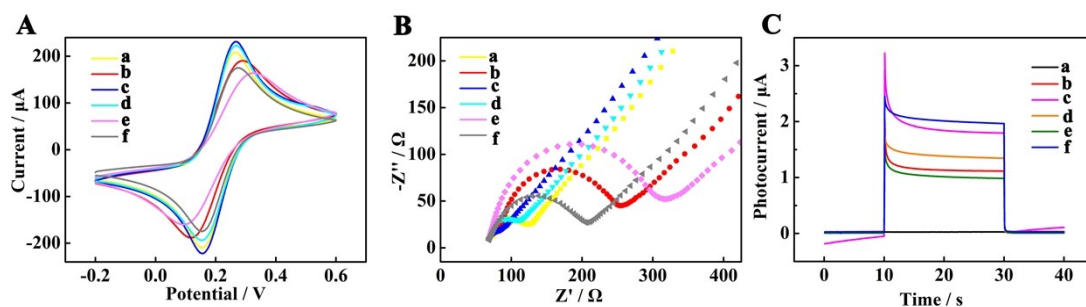


**Figure S4** The CV (A), EIS (B) and PEC (C) responses of (a) bare GCE, (b)  $\text{Ti}_3\text{C}_2/\text{BiVO}_4/\text{GCE}$ , (c) Au NPs/ $\text{Ti}_3\text{C}_2/\text{BiVO}_4/\text{GCE}$ , (d) HP1/Au NPs/ $\text{Ti}_3\text{C}_2/\text{BiVO}_4/\text{GCE}$ , (e) HT/HP1/Au NPs/ $\text{Ti}_3\text{C}_2/\text{BiVO}_4/\text{GCE}$ , (f) output DNA/MB/HT/HP1/Au NPs/ $\text{Ti}_3\text{C}_2/\text{BiVO}_4/\text{GCE}$

**Table S2** Comparison of different methods for the detection of  $\text{VEGF}_{165}$

Detection method	Detection range	Detection limit	Ref.
Fluorescence	10-800 pM	12 pM	3
Fluorescence	100 pM-160 nM	80 pM	4
enzyme-linked immunosorbent assay	-	30 fM	5
Electrochemiluminescence	0 fM-10 nM	10 fM	6
PEC	100 fM-10 nM	30 fM	7
PEC	100 fM-10 nM	30 fM	8
PEC	10 fM-100 nM	3.3 fM	This work

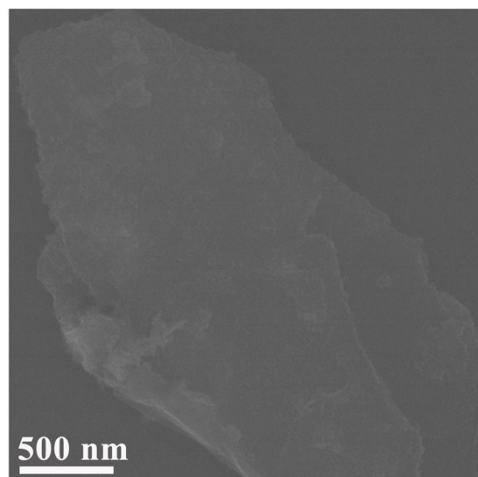


Figure S5 SEM image of  $\text{Ti}_3\text{C}_2$

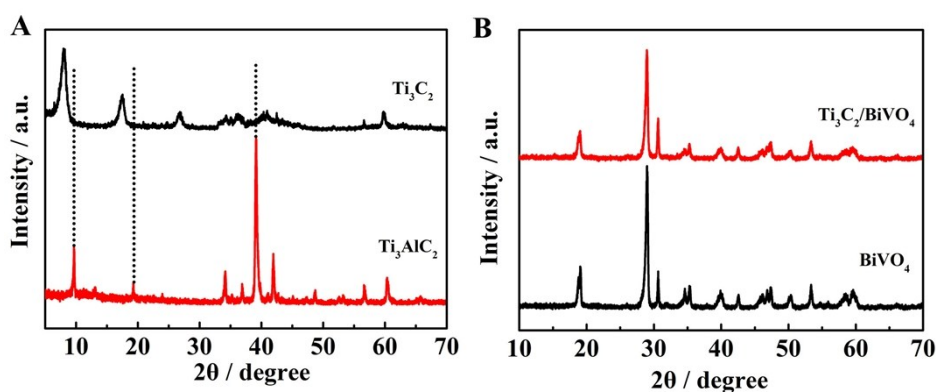


Figure S6 XRD patterns of (A)  $\text{Ti}_3\text{C}_2$  and  $\text{Ti}_3\text{AlC}_2$ ; (B)  $\text{BiVO}_4$  and  $\text{Ti}_3\text{C}_2/\text{BiVO}_4$

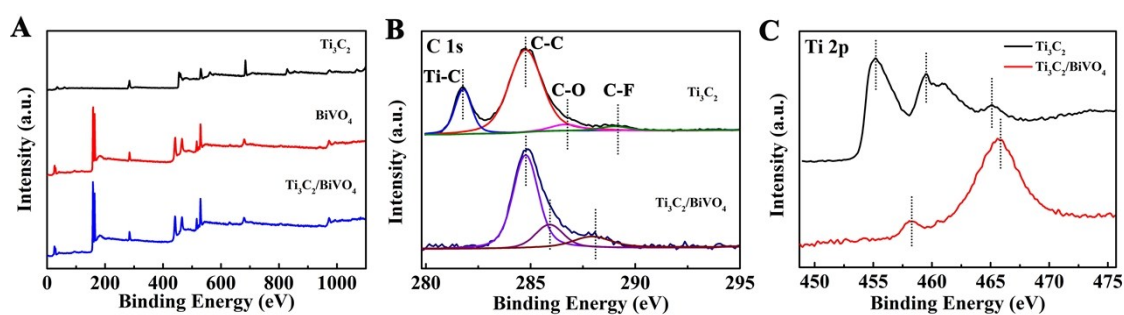
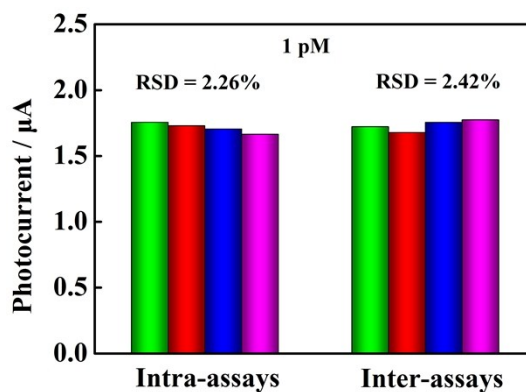


Figure S7 (A) Survey XPS spectrum of  $\text{Ti}_3\text{C}_2$ ,  $\text{BiVO}_4$  and  $\text{Ti}_3\text{C}_2/\text{BiVO}_4$ . High-resolution XPS spectrum of C 1s (B) and Ti 2p (C) of  $\text{Ti}_3\text{C}_2$  and  $\text{Ti}_3\text{C}_2/\text{BiVO}_4$ .



**Figure S8** Reproducibility of the proposed PEC biosensor

#### REFERENCE:

1. Cao, S. W.; Shen, B. J.; Tong, T.; Fu, J. W.; Yu, J. G.; *Adv. Funct. Mater.* 2018, **28**, 1800136.
2. Wang, H.; Sun, Y. M.; Wu, Y.; Tu, W. G.; Wu, S. Y.; Yuan, X. Z.; Zeng, G. M.; Xu, Z. C. J.; Li, S. Z.; Chew, J. W. *Applied Catalysis B: Environmental* 2019, **245**, 290-301.
3. F. M. Moghadam, M. Rahaie, *Biosensors and Bioelectronics*, 2019, **132**, 186-195.
4. D. Zhu, W. Li, H. M. Wen, S. Yu, Z. Y. Miao, A. Kang, A. H. Zhang, *Biosensors and Bioelectronics*, 2015, **74**, 1053-1060.
5. Z. T. Zhao, M. A. Al-Ameen, K. Duan, G. Ghosh and J. F. Lo, *Biosens. Bioelectron.*, 2015, **74**, 305–312.
6. H. Zhang, M. X. Li, C. H. Li, Z. H. Guo, H. L. Dong, P. Wu, C. X. Cai, *Biosensors and Bioelectronics*, 2015, **74**, 98-103.
7. H. M. Da, Y. L. Liu, M. J. Li, R. Yuan, H. Y. Liu, Y. Q. Chai, *Chem. Commun*, 2019, **55**, 8076-8078.

8. H. M. Da, H. Y. Liu, Y. N. Zheng, R. Yuan, Y. Q. Chai, *Biosensors and Bioelectronics*, 2018, **101**, 213-218.